

Research Article

Estimation and Validation of Collection 6 Moderate Resolution Imaging Spectroradiometer Aerosol Products for East Asia

Kwon-Ho Lee*

Department of Atmospheric and Environmental Sciences (DAES), Gangneung-Wonju National University (GWNU), Gangneung 25457, Republic of Korea

***Corresponding author.**

Tel: +82-33-640-2319
E-mail: kwonho.lee@gmail.com

Received: 30 March 2018

Revised: 13 May 2018

Accepted: 15 May 2018

ABSTRACT The operational aerosol retrieval algorithm for the Moderate Resolution Imaging Spectroradiometer (MODIS) measurements was recently updated and named collection 6 (C6). The C6 MODIS aerosol algorithm, a substantially improved version of the collection 5 (C5) algorithm, uses an enhanced aerosol optical thickness (AOT) retrieval process consisting of new surface reflection and aerosol models. This study reports on the estimation and validation of the two latest versions, the C5 and C6 MODIS aerosol products over the East Asian region covering 20°N to 56°N and 80°E to 150°E. This study also presents a comparative validation of the two versions (C5 and C6) of algorithms with different methods (Dark Target (DT) and Deep Blue (DB) retrieval methods) from the Terra and Aqua platforms to make use of the Aerosol Robotic Network (AERONET) sites for the years 2000-2016. Over the study region, the spatially averaged annual mean AOT retrieved from C6 AOT is about 0.035 (5%) less than the C5 counterparts. The linear correlations between MODIS and AERONET AOT are $R = 0.89$ (slope = 0.86) for C5 and $R = 0.95$ (slope = 1.00) for C6. Moreover, the magnitude of the mean error in C6 AOT—the difference between MODIS AOT and AERONET AOT—is 40% less than that in C5 AOT.

KEY WORDS MODIS, Aerosol retrieval, AOT, Satellite, Sun-sky radiometer

1. INTRODUCTION

Estimating the distribution, variation, and intensity of atmospheric aerosols has been an important issue in air quality and climate change studies (Myhre *et al.*, 2013). Several studies have been conducted around the world to understand the impact of atmospheric aerosols, but accurate evaluation of their effects is still challenging due to inhomogeneous aerosol loading and spatio-temporal distribution (e.g., Bellouin *et al.*, 2013; Yang *et al.*, 2009; Huebert *et al.*, 2003; Griggs and Noguera, 2002; Haywood *et al.*, 1999). Thus, fully understanding the impact of aerosol particles on local and global environments is required for evaluation of its characteristics.

The atmospheric environment in East Asia has been affected by severe air pollution originating from human activity and natural aerosols such as desert dust, smoke from forest fire, and biomass burning (Li *et al.*, 2007a; Lee *et al.*, 2006;

Murayama *et al.*, 2004), as westerly winds frequently transport the severe air pollution from the East Asian continent to far distances. Although ground-based observations or airborne measurements can provide aerosol properties in-situ, experimental maintenance as well as point measurements at a fixed location still exist as limitations. Instead, satellite remote sensing has been used to provide a spatial distribution of aerosol optical properties in several studies (e.g., Herman *et al.*, 1997; Kaufman *et al.*, 1997a; Stowe *et al.*, 1997; Tanré *et al.*, 1997). They found that columnar aerosol properties, such as aerosol optical thickness (AOT or τ), integrated from the vertical profiles of aerosol extinction coefficients, can be estimated based on numerical and physical computation.

Due to the large variability in atmospheric constituents and surface properties, retrieval of aerosols from satellite data in the visible wavelength region is an ill-posed problem. To separate the surface from other atmospheric contributions to the satellite-receiving radiances, most algorithms use the dark surface method, which assumes a ground target with very low reflection (Kaufman *et al.*, 1997b). For example, typical vegetation pixels are dark in the red (wavelength $\approx 0.66 \mu\text{m}$) and blue (wavelength $\approx 0.47 \mu\text{m}$) wavelengths, and it is reasonable to use the dark (or low reflection) surface pixels for aerosol retrieval.

Many studies have used various techniques, developed to retrieve aerosols using different satellite sensors with optimized algorithms, and they were reviewed by King *et al.* (1999), Lee *et al.* (2009), and Kokhanovsky and de Leeuw (2009). Well known algorithms for the sensors include the UV-based algorithm for the Total Ozone Mapping Spectroradiometer (TOMS) (Herman *et al.*, 1997), single or dual visible band algorithm for the Advanced Very High-Resolution Radiometer (AVHRR) (Stowe *et al.*, 2002), angular measurement algorithm for the Multiangle Imaging Spectroradiometer (MISR) (Diner *et al.*, 2008; Kahn *et al.*, 2005), ocean color algorithm for the sea-viewing wide field of view sensor (SeaWiFS) (Hsu *et al.*, 2004), and multi-spectral algorithm for the Moderate Resolution Imaging Spectroradiometer (MODIS) (Remer *et al.*, 2005; Kaufman *et al.*, 1997a). Among these aerosol products, MODIS aerosol products have been continuously developed with improved validation schemes. In general, MODIS-retrieved AOT retrievals against the global ground-based measurements from the Aerosol Robotic Network (AERONET) (O'Neill *et al.*, 2005; Dubovik *et al.*, 2002; Dubovik and King, 2000; Holben *et al.*, 1998) showed good agreement (Chu *et al.*, 2002; Ichoku *et al.*, 2002). However, over heavy polluted regions or complex land covered areas, MODIS tends to under- or over-estimate AOT values (i.e., Li *et al.*, 2007b).

The main objectives of this study are to estimate the most recent versions of MODIS aerosol products and to evaluate the discrepancies between satellite products and ground observations. We also investigated the influence factor, which can affect the reliability of aerosol retrieval in the study area. Given the spatio-temporal information of aerosols with an update version of the retrieval algorithm, the understanding and application of satellite-retrieved products will be enhanced. This study is structured as follows. The datasets and methodology employed are explained in section 2. Section 3 compares the two latest versions of the MODIS

Table 1. Specifications of MODIS level 2 aerosol products used in this study.

Characteristics	Collection 5	Collection 6
^{a)} PGE	5.1.0.11	6.0.42
Version	5.1	6.0
Period (used here)	2000-2016	2002-2016
No. of Files	77,491 (Terra)	51,309 (Terra)
	67,476 (Aqua)	44,640 (Aqua)
Total size	87.57 GB (Terra)	81.57 GB (Terra)
	77.33 GB (Aqua)	78.25 GB (Aqua)
Reference	Remer <i>et al.</i> (2005)	Levy <i>et al.</i> (2013)

^{a)} PGE: The Program Executable

Table 2. Characterized parameters of MODIS aerosol retrieval algorithms by dark target (DT) and deep blue (DB) methods.

Parameters	Dark target (DT)	Deep blue (DB)
Region	Land, ocean	Land only
Surface reflectance	SWIR to visible reflectance ratios	Maps and libraries
Best place over	Dark vegetated targets	Bright land surfaces
Spatial resolution of band used	500 m/pixels	1 km/pixels
Spatial resolution of product	3 km and 10 km	10 km
Reference	Levy <i>et al.</i> (2013)	Hsu <i>et al.</i> (2013)

aerosol products. Section 4 presents comparisons between satellite retrievals and ground measurements. We discuss our results and summarize our findings in Section 5.

2. DATA AND METHODOLOGY

The MODIS instrument is a multi-spectral sensor onboard the Terra and Aqua satellites. The Terra and Aqua satellites were launched in December 1999 and

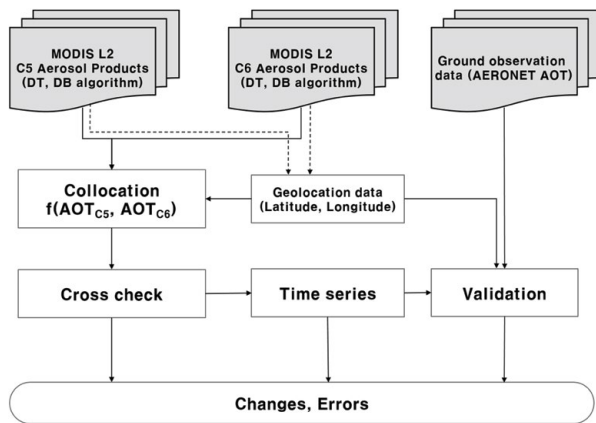


Fig. 1. Schematic diagram of the data processing with MODIS L2 aerosol products.

May 2002, respectively. The Terra satellite is on a descending orbit flying southward across the equator around 01:30 UTC, while the Aqua satellite is on an ascending orbit flying northward around 04:30 UTC. These observation tracks can observe the same place in the morning and afternoon. MODIS has 36 spectral bands ranging from 0.41 μm to 14 μm at three different spatial resolutions (250 m, 500 m, and 1000 m). Three of the spectral bands (i.e., 0.47 μm , 0.66 μm , and 2.12 μm) are used to retrieve aerosols parameters over land, while the remaining bands are used to retrieve aerosol parameters over ocean and for cloud masking and snow cover masking (Remer *et al.*, 2005; Kaufman *et al.*, 1997a).

The most recent MODIS aerosol retrieval algorithm developed are two distinct products denoted as Collections 5 (C5) AOT (Levy *et al.*, 2007; Remer *et al.*, 2005) and Collections 6 (C6) AOT (Levy *et al.*, 2013). Both aerosol products provide global aerosol data retrieved from Terra and Aqua platforms with an expected uncertainty of $\pm 0.05 \pm 0.15\tau$ over land (Tanré *et al.*, 1997) and $\pm 0.03 \pm 0.05\tau$ over ocean (Remer *et al.*, 2005). The C6 AOT dataset generated with the upgraded algorithm increased the global accuracy and coverage without major changes to the basic principles of the algorithm (Levy *et al.*, 2013). Global datasets are generally met within the expected accuracy; however, significantly larger errors are found in local areas (Li *et al.*, 2009; Levy *et*

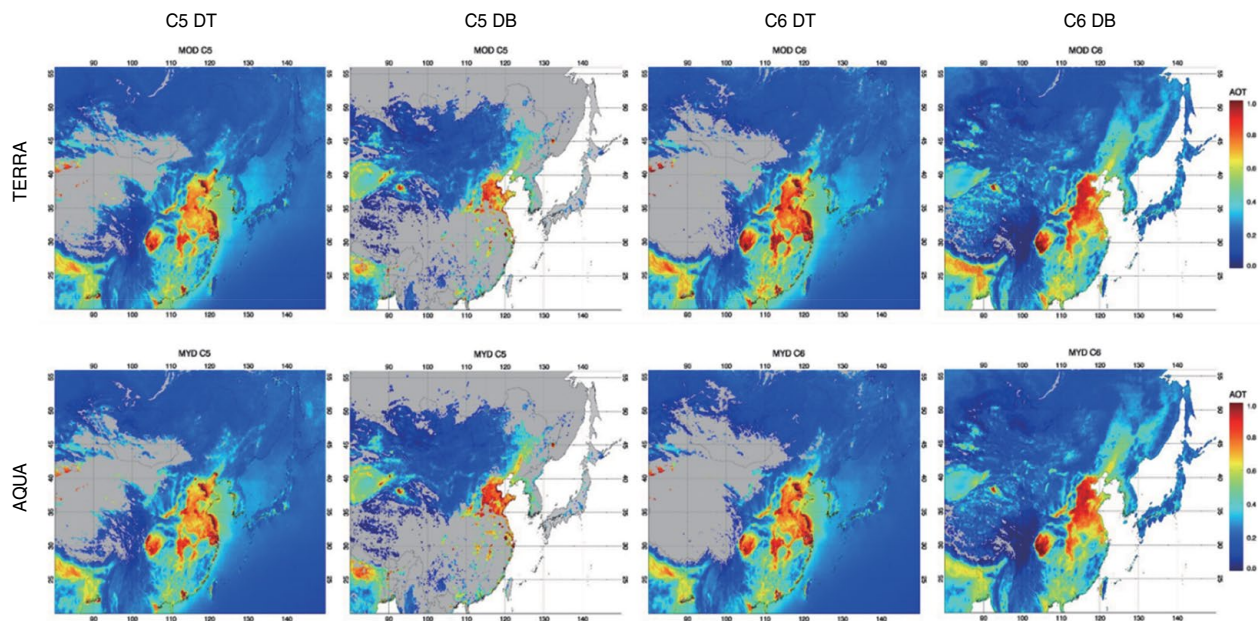


Fig. 2. Averaged spatial distribution of AOT from different collections and retrieval algorithms for MODIS L2 aerosol products during 2000-2015 (Terra) and 2002-2015 (Aqua). Note that the AOT data from DB algorithm are available over land only.

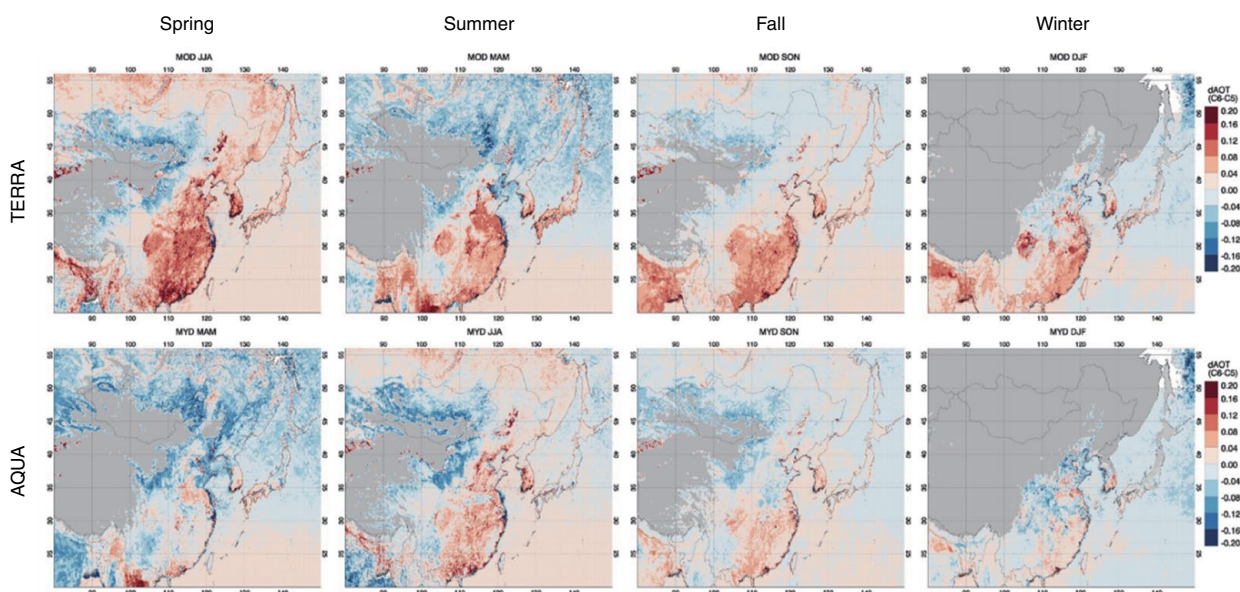


Fig. 3. Absolute difference between the seasonal mean MODIS AOT of different versions (C6 AOT - C5 AOT) by DT algorithm.

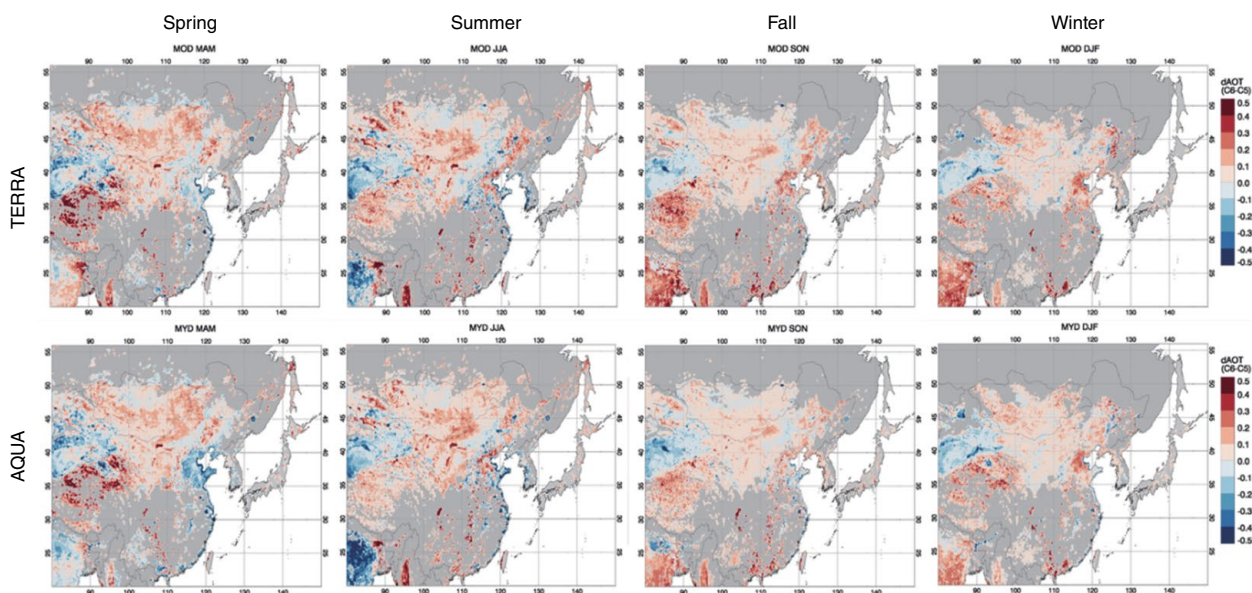


Fig. 4. Absolute difference between the seasonal mean MODIS AOT (C6 AOT - C5 AOT) by DB algorithm.

al., 2005; Remer et al., 2005; Chu et al., 2002). Moreover, in regions without ground measurements for the inter-comparisons, those errors are largely unknown.

In this study, we used two different MODIS aerosol data (Terra and Aqua), generated by two different retrieval methods (dark target (DT) and deep blue (DB)), for the estimation of differences between the C5 and C6 aerosol products. Differences in DT and DB methods

are following. DT has separate algorithms for land and ocean but DB is limited for a land retrieval only. Two methods have different ways of accounting for the surface reflectance. Because aerosol retrieval from satellite observation must account for the surface reflectance to remove its contribution to satellite receiving signal. DT uses spectral ratios between the 0.47, 0.67 and 2.1 μm channels because SWIR channel has lower atmospheric

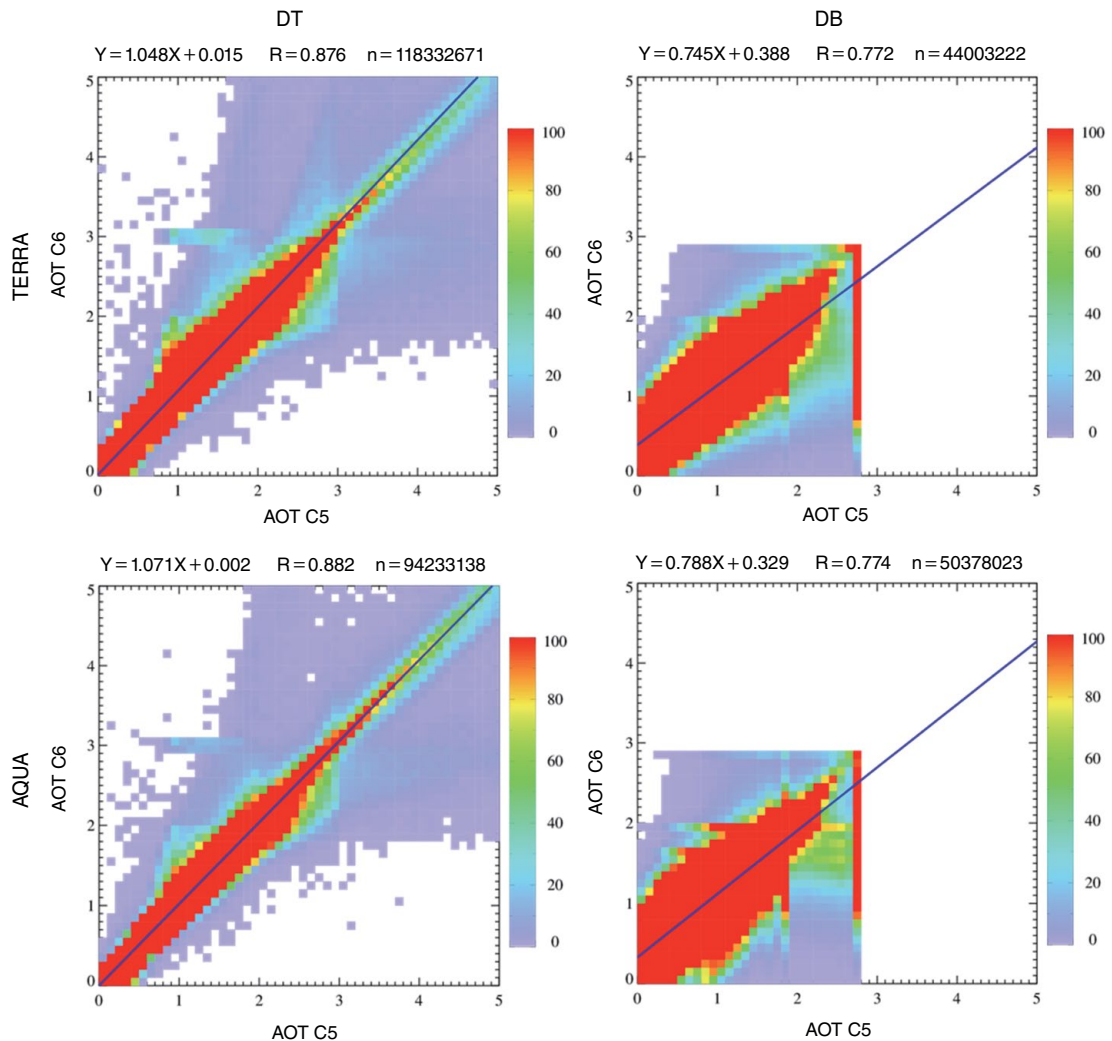


Fig. 5. Scatter plots between MODIS C5 and C6 AOT pixels during 2000-2016 for Terra and 2002-2016 for Aqua. Color scale represents frequency at the given AOT range (highest value means 0.001% and 0.01% of total number of pixels for Terra and Aqua, respectively).

reflection and highly correlated with visible channel. It has known that DT method works best over dark vegetated area and DB works best over bright land surfaces. Since the DT algorithm has limitations for aerosol retrieval over bright land surfaces, the DB algorithm was developed based on the use of the surface reflectance libraries in two blue channels (i.e., $0.412\ \mu\text{m}$ and $0.47\ \mu\text{m}$), where the surface reflection remains very low and largely stable even over bright surfaces (Hsu *et al.*, 2006, 2004). This method works best over bright land surfaces but can also retrieve aerosols over most vegetated targets. More parameters used in DT and DB method are listed in Table 2.

The data used are extracted from MODIS Level 2 (code names: MOD04 for Terra and MYD04 for Aqua)

daily products observed from March 2000 (Jan 2002 for Aqua) to October 2016. It is noteworthy that C5 DB aerosol products are currently available for 2002-2011 from Aqua and 2000-2007 from Terra, based on known calibration issues. The DB algorithm has an expected error of $\pm 0.05 \pm 0.20\tau$ over land (Hsu *et al.*, 2013). Our study region extends from 20°N to 58°N and from 80°E to 150°E , as listed in Table 1. A total of 153,195 C5 datasets and 95,949 C6 datasets were analyzed for the AOT by DT method (hereafter, AOT_{DT}) and by DB method (hereafter, AOT_{DB}), to assess their spatial and temporal (seasonal and year-by-year) variability over the study region.

The MODIS L2 aerosol data products and methods for both versions were validated against corresponding

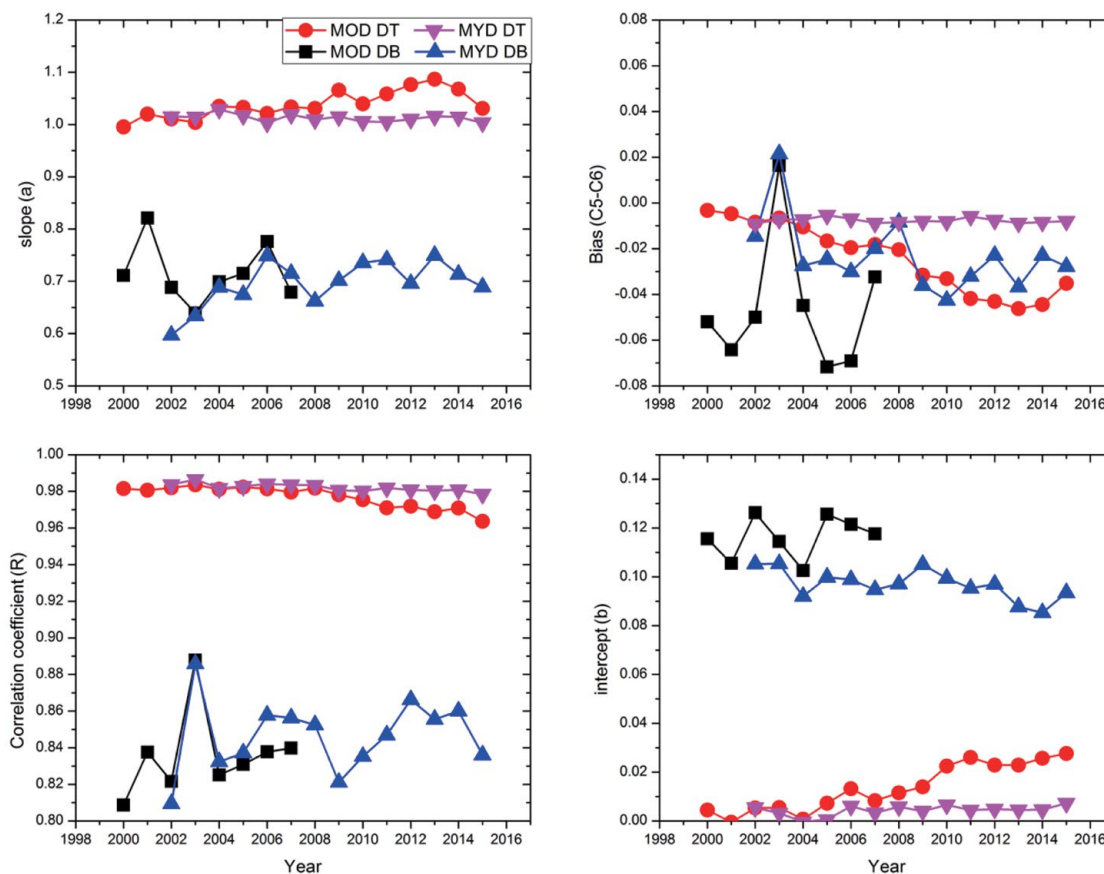


Fig. 6. Inter-annual variations of linear regression slopes, intercepts, correlation coefficients, and mean biases derived from Terra (red and black) and Aqua (magenta and blue) MODIS for the period 2000-2016 over East Asia.

ground-based sun-sky radiometer measurements from the AERONET database (<https://aeronet.gsfc.nasa.gov>). The available AERONET observation sites cover a large part of the East Asian region, with 117 stations within the study area. We used Level 2 cloud-screened and quality-assured data. The overall uncertainty in the AERONET AOT data is known to be ± 0.01 for wavelengths greater than 440 nm and ± 0.02 for shorter wavelengths (Eck *et al.*, 1999).

As shown in Fig. 2, the data analysis process is composed of three parts. First, a valid pair of C5 and C6 data was found for a given pixel at a satellite’s observation time. Both versions of aerosol products including AOT_{DT} and AOT_{DB} are sampled. Second, C5 and C6 data were directly compared to estimate spatial distributions and statistical correlations. Finally, datasets were compared to ground-based AOT measured by sun-skyradiometer for the evaluation of each product.

3. RESULTS

3.1 Comparisons between Collection 5 and Collection 6 Aerosol Products

Fig. 2 shows the 17-year (2000-2016) Terra and 15-year (2002-2016) Aqua MODIS mean AOT for different algorithms and collections. Note that lots of missing data points expressed as grey area over land are bright land surface features, such as deserts or urban areas in the C5/C6 DT algorithm. Over the bright land surface, there is no retrieval for AOT_{DT} , but pixels are available in AOT_{DB} . Furthermore, AOT_{DB} products are only available over land. After expanding the region of interest in the C6 DT method, more effective data numbers are currently available than any other products over land. In general, mean AOT values range from 0.1 to 1.0 at 550 nm, exhibiting an increase in the continent. Larger AOT values (AOT up to 1.0 at 550 nm over the populated region and megacities), reflecting a significant aerosol

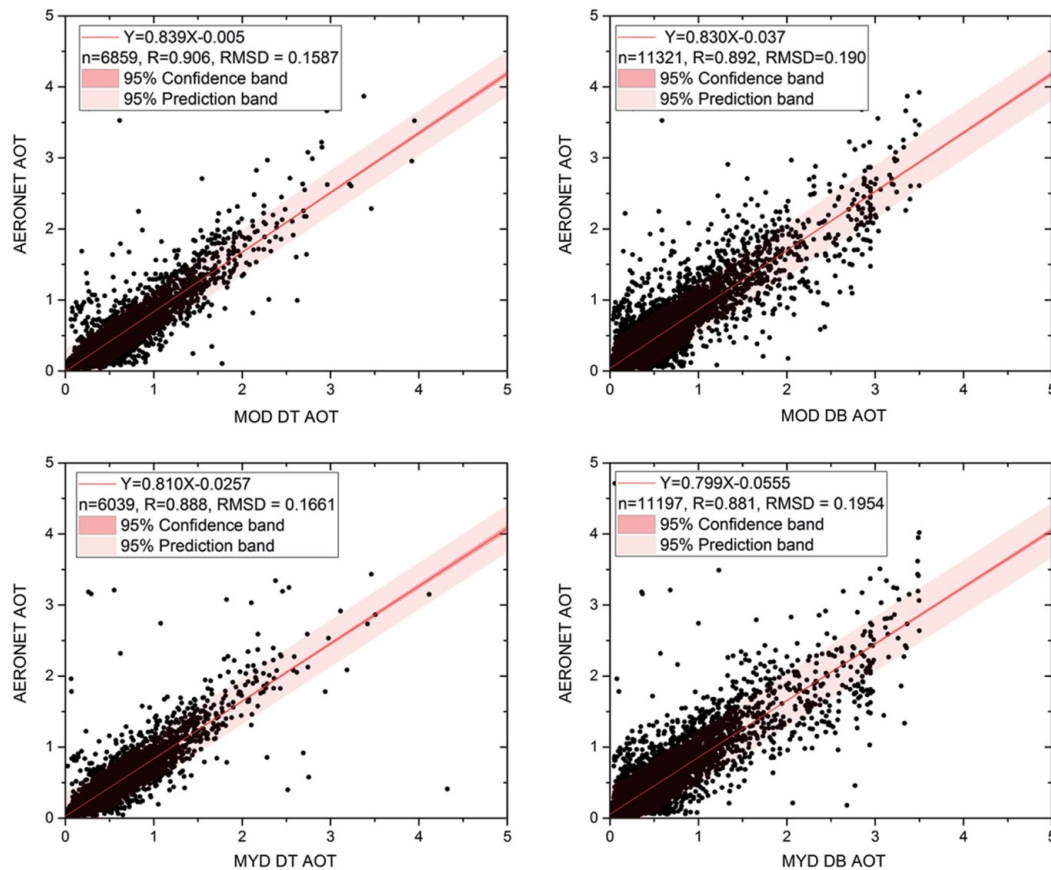


Fig. 7. Terra and Aqua C6 MODIS AOT products plotted against collocated AERONET observations. The solid straight lines represent the linear regression fit to the collocating data points and the corresponding regression coefficients of the linear fit are also shown in each panel.

load, are observed mainly in the eastern parts of China originating from nearby great urban and industrial areas. The C6 AOT_{DT} distribution is in agreement with that of C5 AOT_{DT}, reported by previous studies (Levy *et al.*, 2013). However, large disagreement is found in the DB algorithms over the study areas, where the C5 AOT_{DB} values are not consistent with C5 AOT_{DT} areas. C6 AOT_{DB} products cover almost the entire land area and their distributions are reasonable. Again, the C6 DB algorithm expands its coverage to vegetated regions, whereas the C5 DB algorithm is limited to bright surfaces only.

The distributions of the seasonal mean differences of AOT from C6 and C5 ($dAOT_{C6-C5} = C6 \text{ AOT} - C5 \text{ AOT}$) generated by different algorithms (DT and DB) during the entire study period is mapped in Figs. 3 and 4. For the DT algorithm, as shown in Fig. 3, large negative values of $dAOT_{C6-C5}$ (< -0.25) occur over east-central China in spring and summer, but the lowest

$dAOT_{C6-C5}$ values ($\sim \pm 0.01$) occur over southern China and the ocean. For the DB algorithm, as shown in Fig. 4, $dAOT_{C6-C5}$ shows negative differences ranging from -20% to -50% over almost half the land surface in the study area. Overall, the C6 AOT retrievals are greater than the C5 retrievals, as seen more clearly in the scatterplots of Figs. 5 and 6. These results are similar to the previous study using the MODIS Collection 4 (C4) and C5 aerosol products (Li *et al.*, 2007b).

To facilitate the comparison of four different MODIS aerosol products (C5 AOT_{DT}, C6 AOT_{DT}, C5 AOT_{DB}, and C6 AOT_{DB}), the data were sampled by corresponding geographic latitudes and longitudes. Fig. 5 shows the relationship between C5 and C6 AOT with DT and DB algorithms. Although the C5 and C6 AOT products were not made in the same location for entire study areas, existing collocated pixel data were compared at the same time. In the left column of Fig. 5, these two versions of AOT_{DT} products have slight differences in their

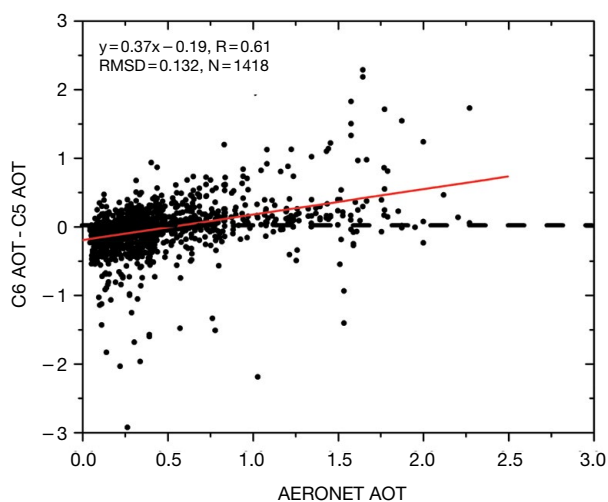


Fig. 8. Scatter plots of MODIS (C6 AOT - C5 AOT) versus AERONET AOT.

magnitude. For AOT_{DT} values greater than 3.0, a greater number of scattered data points means that the two aerosol retrieval results are quite different due to their algorithms. C6 AOT_{DT} values are slight larger than the C5 AOT_{DT} values, as seen more clearly in these scatterplots. This overestimation of C5 from the algorithm is very similar to the results from the former versions, regarding the differences between C5 and C4 studied in Li *et al.* (2007b). For AOT_{DB} products, as shown in the right column of Fig. 5, AOT_{DB} products have substantial differences that are larger than those in the AOT_{DT} cases. It is noteworthy that the maximum permitted AOT_{DT} is 5.0, and in AOT_{DB} the limit is as low as 3.5 over the globe. Moreover, it was found that the largest C6 AOT_{DB} values were 2.75 for C5 and 2.88 for C6 in these comparisons. About 42.8% of C5 AOT_{DB} samples were larger than those of C6 AOT_{DB} . In general, relatively high correlations were found to have moderate correlation coefficients of ~ 0.88 and ~ 0.77 for C5 versus C6 AOT_{DT} and AOT_{DB} retrievals, respectively. The slightly weak correlation coefficient for the AOT_{DB} retrieval is due to the smaller number of data points, different surface reflection scheme, and aerosol assumptions in the look-up tables used (Hsu *et al.*, 2013).

During the yearly observation period, the paired data points of Terra/Aqua MODIS C5 and C6 with AOT_{DT} and AOT_{DB} retrievals have been fitted, and linear regression lines and the corresponding statistical coefficients such as slope, y-intercept, correlation coefficient (R), and bias were obtained. These statistical results are

shown in Fig. 6. These results revealed that the variability in AOT values derived from the different version is similar for AOT_{DT} retrievals but large for AOT_{DB} retrievals. It is also noted that the C5 AOT_{DT} derived from the Aqua MODIS sensor followed the pattern most stable and similar to the C6 products during the study period. The results also reveal a rather significant yearly variation in the AOT_{DT} from the Terra MODIS, suggesting that the C6 algorithm reflected the differences in the aerosol's microphysical properties and surface reflection contributions. Meanwhile, over the entire MODIS observation period, the correlation values tend to be larger for AOT_{DB} , but the biases increased with some fluctuations. It is interesting that year 2003 has the largest correlation coefficient, with a positive bias year with AOT_{DB} for both Terra and Aqua MODIS, and bias values of 0.016 for Terra and 0.021 for Aqua. During the study period, each AOT result from the C6 algorithm has a negative bias value, as discussed earlier. These bias values were -0.046 ± 0.028 for AOT_{DB} and -0.024 ± 0.015 for AOT_{DT} in the case of Terra MODIS, and -0.041 ± 0.016 for AOT_{DB} and -0.005 ± 0.016 for AOT_{DT} in the case of Aqua MODIS. The aerosol retrieval products differ because of sensor calibration, processing methods, and retrieval algorithms.

3.2 Comparisons between MODIS and AERONET AOTs

This section is based on the comparisons of MODIS aerosol products discussed in the former sections and AERONET AOT (hereafter, AOT_{AN}) for evaluation in the study area. In these comparisons, the quality-assured level 2.0 AOT_{AN} data with a known uncertainty of 0.015 (Holben *et al.*, 1998) were used as the ground truth data. AOT_{AN} data were collocated in space and time with Terra/Aqua MODIS AOT_{DT} and AOT_{DB} for C5 and C6 algorithms, following the method used in Ichoku *et al.* (2002). Using this collocation method, a pair of MODIS AOT and AOT_{AN} data were sampled when the temporal difference between the two data was found to be within ± 30 min, and the spatial distance was within 25 km. Note that, AOT_{AN} data are not available at 550 nm, so AERONET data from the 0.50 and 0.67 μm spectral channels were interpolated to derive AOT values at the 0.55 μm channel, following O'Neill *et al.* (2003).

The collocated AOT values obtained from the MODIS were validated against the AOT_{AN} over the

study area. In Fig. 5, all MODIS AOT products agree generally well with AOT_{AN} within uncertainty levels for each retrieval algorithm. The slopes and intercepts of linear regression lines obtained from the validation is of vital importance. In the case of Terra and Aqua MODIS, the respective correlation coefficients were observed to be 0.88-0.91 with intercepts of 0.005-0.055. Meanwhile, the slopes of 0.799-0.839 deviate from the ideal state, which indicates that MODIS AOTs are systematically overestimated by 31-40%.

In the following, we will now estimate how the retrieved MODIS AOT from the difference algorithms change with the truth AOT. The difference in MODIS AOT retrievals is an essential parameter in estimating the reliable quality of the retrieved AOT products. The relationship between this difference in MODIS AOT retrievals and the AOT_{AN} is illustrated in Fig. 8. One can see that the MODIS C6-C5 difference increases with AOT_{AN} . Consequently, the variation in the MODIS C6-C5 difference with AOT_{AN} suggests that there are issues with the assumed scattering properties of the aerosol types in MODIS aerosol retrieval algorithms.

4. SUMMARY AND CONCLUSIONS

The first MODIS observations for atmospheric aerosols were made in early 2000. These MODIS observations provide continuous global coverage and has helped improve retrieval of aerosol products. Such observations are required for satellite data interpretation. Recently, the MODIS aerosol retrieval algorithm was modified and revised, denoted as C6, and a new version of aerosol product was generated to replace the former C5 product. Using MODIS level 2 aerosol product from the most available C5 and C6 from the Terra and Aqua MODIS dataset, we estimated the spatio-temporal variations of the AOT over East Asia during the period from 2000 to 2016. Because the study area is one of the important aerosol sources such as desert dust, urban/industrial emissions, and biomass burning, qualified and quantified aerosol remote sensing data are helpful in understanding their distributions and intensities.

Generally, higher AOT values were observed offshore in east-central China with the maximum values being over the study area. The results confirm that previous MODIS C5 AOT distributions have less spatial coverage, and they exhibit large differences with the current

C6 AOT. Two versions of the AOT_{DT} products have slight differences. For MODIS AOT_{DB} , these differences were demonstrated in the regression analysis through smaller slopes and intercepts, and lower correlation coefficients. Although the DB algorithm expands its coverage from the limited bright surface in C5 to vegetated regions in C6, the C5-C6 differences range from -20% to -50% over almost half of land surface in the study area. The moderate correlations were found to be correlation coefficients of 0.876 and 0.76 for C5 versus C6 AOT_{DT} and AOT_{DB} retrievals, respectively. These results are due to a fewer number of data points, different surface reflection scheme, and aerosol optical properties used in the LUT.

Comparisons between the MODIS AOT products with AOT_{AN} confirm that the error ranges of MODIS aerosol products were within the uncertainty levels for each retrieval algorithm. Linear regression analysis showed that the respective correlation coefficients were observed to be 0.88 - 0.91, with intercepts of 0.005 - 0.055. Meanwhile, the slopes of 0.799 - 0.839 deviate from the ideal state, which indicates that MODIS AOTs are systematically overestimated by 31 - 40%. Also, the difference in MODIS AOT retrievals from the two versions increase with ground truth AOT. Consequently, these estimation and validation results with C5 and C6 retrieval products suggest that there are issues with the assumed scattering properties of the aerosol types in MODIS aerosol retrieval algorithms.

ACKNOWLEDGEMENT

This work was supported by the Korea Meteorological Administration Research and Development Program under Grant KMIPA2015-2012. The MODIS L2 aerosol products were acquired from the Level-1 and Atmosphere Archive & Distribution System (LAADS) Distributed Active Archive Center (DAAC), located in the Goddard Space Flight Center in Greenbelt, Maryland (<https://ladsweb.nascom.nasa.gov/>). We acknowledge and appreciate the AERONET program and their contributing principal investigators and staff for establishing and maintaining the sites used in this investigation.

REFERENCES

Bellouin, N., Quaas, J., Morcrette, J.-J., Boucher, O. (2013)

- Estimates of aerosol radiative forcing from the MACC reanalysis. *Atmospheric Chemistry and Physics* 13, 2045-2062.
- Chu, D.A., Kaufman, Y.J., Ichoku, C., Remer, L.A., Tanré, D., Holben, B.N. (2002) Validation of MODIS aerosol optical depth retrieval overland. *Geophysical Research Letters* 29, doi:10.1029/2001GL013205.
- Diner, D.J., Abdou, W.A., Ackerman, T.P., Crean, K., Gordon, H.R., Kahn, R.A., Martonchik, J.V., McMuldroy, S., Paradise, S.R., Pinty, B., Verstraete, M.M., Wang, M., West, R.A. (2008) MISR level 2 aerosol retrieval algorithm theoretical basis. Jet Propulsion Laboratory Pasadena, CA, JPL-D 11400, Rev. G.
- Dubovik, O., King, M.D. (2000) A flexible inversion algorithm for retrieval of aerosol optical properties from Sun and sky radiance measurements. *Journal of Geophysical Research* 105, 20673-20696.
- Dubovik, O., Holben, B.N., Eck, T.F., Smirnov, A., Kaufman, Y.J., King, M.D., Tanré, D., Slutsker, I. (2002) Variability of absorption and optical properties of key aerosol types observed in worldwide locations. *Journal of Atmospheric Science* 59, 590-608.
- Eck, T.F., Holben, B.N., Reid, J.S., Dubovik, O., Smirnov, A., O'Neill, N.T., Slutsker, I., Kinne, S. (1999) Wavelength dependence of the optical depth of biomass burning, urban and desert dust aerosols. *Journal of Geophysical Research* 104, 31333-31349.
- Griggs, D.J., Noguer, M. (2002) Climate change 2001: the scientific basis. Contribution of working group I to the third assessment report of the intergovernmental panel on climate change. *Weather* 57, 267-269.
- Haywood, J., Ramaswamy, V., Soden, B. (1999) Tropospheric aerosol climate forcing in clear-sky satellite observations over the oceans. *Science* 283, 1299-1303.
- Herman, J.R., Bhartia, P.K., Torres, O., Hsu, C., Seftor, C., Celarier, E. (1997) Global distribution of UV-absorbing aerosols from Nimbus 7/TOMS data. *Journal of Geophysical Research* 102, 16911-16922.
- Holben, B.N., Eck, T.F., Slutsker, I., Tanré, D., Buis, J.P., Setzer, A., Vermote, E., Reagan, J.A., Kaufman, Y.J., Nakajima, T., Lavenu, F., Jankowiak, I., Smirnov, A. (1998) AERONET-a federated instrument network and data archive for aerosol characterization. *Remote Sensing Environment* 66, 1-16.
- Hsu, C.N., Tsay, S.C., King, M.D., Herman, J.R. (2004) Aerosol properties over bright-reflecting source regions. *IEEE Transactions on Geoscience and Remote Sensing* 42, 557-569.
- Hsu, C.N., Tsay, S.C., King, M.D., Herman, J.R. (2006) Deep blue inversions of Asian aerosol properties during ACE-Asia. *IEEE Transactions on Geoscience and Remote Sensing* 44, 3180-3195.
- Hsu, N.C., Jeong, M.-J., Bettenhausen, C., Sayer, A.M., Hansell, R., Seftor, C.S., Huang, J., Tsay, S.-C. (2013) Enhanced deep blue aerosol retrieval algorithm: The second generation. *Journal of Geophysical Research: Atmospheres* 118, 9296-9315.
- Huebert, B.J., Bates, T., Russell, P.B., Shi, G., Kim, Y.J., Kawamura, K., Carmichael, G., Nakajima, T. (2003) An overview of ACE-Asia: Strategies for quantifying the relationships between Asian aerosols and their climatic impacts. *Journal of Geophysical Research: Atmospheres* 108, 1984-2012.
- Ichoku, C., Chu, D.A., Mattoo, S., Kaufman, Y.J., Remer, L.A., Tanré, D., Slutsker, I., Holben, B.N. (2002) A spatio-temporal approach for global validation and analysis of MODIS aerosol products. *Geophysical Research Letters* 29, 1616-1619.
- Kahn, R.A., Gaitley, B.J., Martonchik, J.V., Diner, D.J., Crean, K.A., Holben, B. (2005) Multiangle Imaging Spectroradiometer (MISR) global aerosol optical depth validation based on 2 years of coincident Aerosol Robotic Network (AERONET) observations. *Journal of Geophysical Research* 110, D10S04, doi:10.1029/2004JD004706.
- Kaufman, Y.J., Tanré, D., Remer, L., Vermote, E.F., Chu, A., Holben, B.N. (1997a) Operational remote sensing of tropospheric aerosol over land from EOS moderate resolution imaging spectrometer. *Journal of Geophysical Research* 102, 17051-17067.
- Kaufman, Y.J., Wald, A.E., Remer, L.A., Gao, B.-C., Li, R.-R., Flynn, L. (1997b) The MODIS 2.1-mm channel correlation with visible reflectance for use in remote sensing of aerosol. *IEEE Transactions on Geoscience and Remote Sensing* 35, 1286-1298.
- King, M.D., Kaufman, Y.J., Tanré, D., Nakajima, T. (1999) Remote sensing of tropospheric aerosols from space: Past, present, and future. *Bulletin of the American Meteorological Society* 80, 2229-2259.
- Kokhanovsky, A.A., de Leeuw, G. (2009) Satellite aerosol remote sensing over land, Springer-Praxis, Berlin, Heidelberg, 379 pp.
- Lee, K.H., Kim, Y.J., Kim, M.J. (2006) Characteristics of aerosol observed during two severe haze events over Korea in June and October 2004. *Atmospheric Environment* 40, 5146-5155.
- Lee, K.H., Li, Z., Kim, Y.J., Kokhanovsky, A. (2009) Atmospheric aerosol monitoring from satellite observations: A history of three decades. In *Atmospheric and Biological Environmental Monitoring* (Kim, Y.J., Platt, U., Gu, M.B. and Iwahashi, H. Eds), Springer, Berlin, Heidelberg, pp. 13-38.
- Levy, R.C., Remer, L.A., Martins, J.V., Kaufman, Y.J., Planafattori, A., Redemann, J., Wenny, B. (2005) Evaluation of the MODIS aerosol retrievals over ocean and land during CLAMS. *Journal of Atmospheric Science* 62, 974-992.
- Levy, R.C., Remer, L.A., Mattoo, S., Vermote, E.F., Kaufman, Y.J. (2007) A second-generation algorithm for retrieving aerosol properties over land from MODIS spectral reflectance. *Journal of Geophysical Research* 112, D13211.
- Levy, R.C., Mattoo, S., Munchak, L.A., Remer, L.A., Sayer, A.M., Hsu, N.C. (2013) The Collection 6 MODIS aerosol products over land and ocean. *Atmospheric Measurement Techniques* 6, 2989-3034.
- Li, Z., Chen, H., Cribb, M., Dickerson, R., Holben, B., Li, C., Lu, D., Luo, Y., Maring, H., Shi, G., Tsay, S.-C., Wang, P., Wang, Y., Xia, X., Zheng, Y., Yuan, T., Zhao, F. (2007a) Preface to special section on East Asian Studies of Tropo-

- spheric Aerosols: An International Regional Experiment (EASTAIRE). *Journal of Geophysical Research* 112, D22S00, doi:10.1029/2007JD008853.
- Li, Z., Niu, F., Lee, K.-H., Xin, J., Hao, W.-M., Nordgren, B., Wang, Y., Wang, P. (2007b) Validation and understanding of Moderate Resolution Imaging Spectroradiometer aerosol products (C5) using ground-based measurements from the handheld Sun photometer network in China. *Journal of Geophysical Research* 112, D22S07. doi:10.1029/2007JD008479.
- Li, Z., Zhao, X., Kahn, R., Mishchenko, M., Remer, L., Lee, K.H., Wang, M., Laszlo, I., Nakajima, T., Marig, H. (2009) Uncertainties in satellite remote sensing of aerosols and impact on monitoring its long-term trend: a review and perspective. *Journal of Annales Geophysicae* 27, 2755-2770.
- Murayama, T., Müller, D., Wada, K., Shimizu, A., Sekiguchi, M., Tsukamoto, T. (2004) Characterization of Asian dust and Siberian smoke with multi-wavelength Raman LIDAR over Tokyo. Japan in spring. 2003. *Geophysical Research Letters* 31, L23103. doi: 10.1029/2004GL021105.
- Myhre, G., Shindell, D., Bréon, F.-M., Collins, W., Fuglestedt, J., Huang, J., Koch, D., Lamarque, J.-F., Lee, D., Mendoza, B., Nakajima, T., Robock, A., Stephens, G., Takemura, T., Zhang, H. (2013) Anthropogenic and Natural Radiative Forcing. In *Climate Change 2013: The Physical Science Basis. Contribution of Working Group I to the Fifth Assessment Report of the Intergovernmental Panel on Climate Change* (Stocker, T.F., Qin, D., Plattner, G.-K., Tignor, M., Allen, S.K., Boschung, J., Nauels, A., Xia, Y., Bex, V. and Midgley P.M. Eds), Cambridge University Press, Cambridge, United Kingdom and New York, NY, USA.
- O'Neill, N.T., Eck, T.F., Smirnov, A., Holben, B.N., Thulasiraman, S. (2003) Spectral discrimination of coarse and fine mode optical depth, *Journal of Geophysical Research* 108, 4559. doi:10.1029/2002JD002975.
- O'Neill, N.T., Thulasiraman, S., Eck, T.F., Reid, J.S. (2005) Robust optical features of fine mode size distributions: Application to the Quebec smoke event of 2002. *Journal of Geophysical Research* 110, D11207, doi:10.1029/2004JD005157.
- Remer, L.A., Kaufman, Y.J., Tanre, D., Mattoo, S., Chu, D.A., Martins, J.V., Li, R.-R., Ichoku, C., Levy, R.C., Kleidman, R.G., Eck, T.F., Vermote, E., Holben, B.N. (2005) The MODIS Aerosol Algorithm, Products and Validation. *Journal of Atmospheric Science* 62, 947-973.
- Stowe, L.L., Ignatov, A.M., Singh, R.R. (1997) Second generation operational aerosol product at NOAA/NESDIS. *Journal of Geophysical Research* 102, 16923-16934.
- Stowe, L.L., Jacobowitz, H., Ohring, G., Knapp, K., Nalli, N. (2002) The Advanced Very High Resolution Pathfinder Atmosphere (PATMOS) climate dataset: Initial analysis and evaluations. *Journal of Climate* 15, 1243-1260.
- Tanré, D., Kaufman, Y.J., Herman, M., Mattoo, S. (1997) Remote sensing of aerosol properties over oceans using the MODIS/EOS spectral radiances. *Journal of Geophysical Research* 102, 16971-16988.
- Yang, M., Howell, S., Zhuang, J., Huebert, B. (2009) Attribution of aerosol light absorption to black carbon, brown carbon, and dust in China-interpretations of atmospheric measurements during EAST-AIRE. *Atmospheric Chemistry and Physics* 9, 2035-2050.